



Published in final edited form as:

*Proteomics*. 2010 August ; 10(15): 2746–2757. doi:10.1002/pmic.200900419.

## Identification of FBXO25-interacting Proteins Using an Integrated Proteomics Approach

Felipe R. Teixeira<sup>1,\*</sup>, Sami Yokoo<sup>1,\*</sup>, Carlos G. Gartner<sup>3</sup>, Adriana O. Manfiolli<sup>1</sup>, Munira M. A. Baqui<sup>2</sup>, Eliana M. Assmann<sup>4</sup>, Ana Leticia G. C. Maragno<sup>1</sup>, Huijun Yu<sup>5</sup>, Primal de Lanerolle<sup>5</sup>, Jörg Kobarg<sup>4</sup>, Steven P. Gygi<sup>3</sup>, and Marcelo D. Gomes<sup>1,§</sup>

<sup>1</sup>Department of Biochemistry and Immunology, University of São Paulo, Ribeirão Preto, Brazil

<sup>2</sup>Department of Cellular and Molecular Biology of the Faculty of Medicine of Ribeirão Preto, University of São Paulo, Ribeirão Preto, Brazil

<sup>3</sup>Cell Biology Department of Harvard Medical School, Harvard University, Boston, USA

<sup>4</sup>Laboratório Nacional de Bociências, Centro Nacional de Pesquisa em Energia e Materiais, Campinas, Brazil

<sup>5</sup>Department of Physiology and Biophysics, University of Illinois at Chicago, Chicago, USA

### Abstract

FBXO25 is one of 68 human F-box proteins that serve as specificity factors for a family of ubiquitin ligases composed of Skp1, Rbx1, Cullin1 and F-box protein (SCF1) that are involved in targeting proteins for destruction across the ubiquitin proteasome system. We recently reported that the FBXO25 protein accumulates in novel subnuclear structures named FBXO25-associated nuclear domains (FANDs). Combining two-step affinity purification followed by mass spectrometry with a classical two-hybrid screen, we identified 132 novel potential FBXO25 interacting partners. One of the identified proteins,  $\beta$ -actin, physically interacts through its N-terminus with FBXO25 and is enriched in the FBXO25 nuclear compartments. Inhibitors of actin polymerization promote a significant disruption of FANDs, indicating that they are compartments influenced by the organizational state of actin in the nucleus. Furthermore, FBXO25 antibodies interfered with RNA polymerase II transcription *in vitro*. Our results open new perspectives for the understanding of this novel compartment and its nuclear functions.

### Introduction

The ubiquitin proteasome system (UPS) plays important roles in a variety of cellular functions, controlling the levels of crucial intracellular regulatory proteins including transcription factors and cell cycle regulatory proteins [1]. UPS protein substrates are targeted for degradation by covalent attachment of ubiquitin (Ub), which is mediated by an enzymatic cascade consisting of three steps involving Ub activating (E1), Ub conjugating (E2) and Ub ligating (E3) enzymes. Subsequently, Ub-conjugated proteins are degraded by the 26S-proteasome complex [2]. E3s are critical players in this system because of their roles in substrate recognition.

<sup>§</sup>Address correspondence to: Marcelo Damário Gomes, Departamento de Bioquímica e Imunologia, Faculdade de Medicina de Ribeirão Preto da USP, Avenida Bandeirantes, 3900, CEP 14049-900 Ribeirão Preto - SP, Brasil, Tel.: (+55) 16-3602-3047, Fax: (+55) 16-3633-6840, mdamario@fmrp.usp.br.

\*F.R.T and S.Y. contributed equally to this work.

The largest family of E3 comprises the cullin-really interesting new gene (RING) complexes whose prototype is the SCF1 complex, composed of the invariable components cullin 1 (CUL1), s-phase-kinase associated protein 1 (Skp1), RING-box 1 (RBX1)/regulator of cullin 1 (ROC1), and an interchangeable component known as an F-box protein (FBP) [3]. In addition to the F-box motif that binds to Skp1, FBP contains distinct protein-protein interaction domains that function in substrate recognition. Posttranslational modifications, such as protein phosphorylation, prolylhydroxylation, or glycosylation are important in regulating interactions of a potential substrate with the FBP [4]. SCF1-mediated ubiquitination is also regulated by mechanisms that involve both site-specific modification of the cullin 1 protein by the small Ub-like protein Nedd8, and CAND1 (cullin-associated Nedd8-dissociated 1)[5-7].

Previously, we demonstrated that the FBXO25, the closest paralog of atrogin-1, has the properties of an E3 of the SCF class [8,9]. Our biochemical studies have indicated that FBXO25 protein was present in all mouse tissues except striated muscle [10]. Furthermore, immunochemical visualization of FBXO25 in cultured cells has revealed that the protein is found in the nucleus, either diffusely spread or arranged in dot-like structures, the FANDs [10]. In the cell nucleus, FANDs are colocalized with the proteasome and ubiquitinated proteins. Interestingly, inhibition of RNA polymerase I disrupted FANDs indicating that they are dynamic structures. In mammalian cells, FANDs recruited polyglutamine-containing proteins and prevented their accumulation in the nucleus [10]. Taken together, these data suggested that FBXO25 is a functional E3 ligase and that FANDs are competent sites of polyubiquitination in the nucleus.

Cells contain a large number of Ub system enzymes and substrates, but relatively few E3s have been examined for their specific targets and regulators [11]. In the present study, we employ a combination of two proteomics approaches, the classical yeast two-hybrid screen and modified tandem affinity purification followed by mass spectrometry analysis, to screen for potential FBXO25-interacting proteins. We show the utility of our strategies through confirmation of known subunits and a regulator of the SCF1, and the identification of various novel FBXO25 interacting proteins. We also report the copurification of  $\beta$ -actin, which appears to play an important role in organizing FBXO25 distribution in the nucleus of HEK293H cells.

## Experimental Procedures

### Materials

Preparation of polyclonal rabbit anti-FBXO25 was described previously [10]. Anti-glutathione S-transferase (GST), anti-actin (clone C4) and anti-CAND1/TIP120A mouse monoclonal antibody (mAbs) were purchased from Santa Cruz Biotechnology Inc, Santa Cruz, CA. Anti-CUL1 was purchased from Upstate Biotechnology Inc., Lake Placid, NY. Anti-Skp1 mouse mAbs, Prolong gold antifade reagent with 4,6-diamidino-2-phenylindole (DAPI), and NuPAGE<sup>®</sup> Bis-Tris 4%–12% gels were obtained from Invitrogen Life Technologies, Carlsbad, CA. Secondary antibodies conjugated with Alexa Fluor 488 and Alexa Fluor 594 were obtained from Invitrogen Life Technologies, Carlsbad, CA. Peroxidase-linked anti-mouse IgG fragment (KPL, Inc., Gaithersburg, MD) and peroxidase-linked goat anti rabbit were produced in-house [10].

### DNA expression constructs

The GATEWAY<sup>™</sup> cloning system constructs pDEST27-HA-FBXO25-FLAG (GST-tagged, full-length, WT) and pDEST27-HA- $\Delta$ F-FBXO25-FLAG (GST-tagged, F-box domain deleted) were described previously [8]. To make F-box deleted ( $\Delta$ F) and truncated (CT1-2)

FBXO25 LexA-tagged fusion constructs, cDNA was amplified using pENTRY-FBXO25 ( $\Delta$ F) described in Maragno et al. [8] as template:  $\Delta$ F-F (5'-GGGAATTCATGCCGTTTCTGGGTCAGG-3'),  $\Delta$ F-R (5'-GGCGGATCCTCAGAAGCTTGAAGAGGTG-3'), CT1-F (5'-GGGAATTCATGCCGTTTCTGGGTCAGG-3'), CT1-R (5'-CCGGATCCTCATTTTTCTGAAAGGATC-3'), CT2-F (5'-GGGAATTCATGCCGTTTCTGGGTCAGG-3'), and CT2-R (5'-CCGGATCCTCATGCTGCCAGCTGAGGAC-3') primers. The products were digested with EcoRI and BamHI and subcloned into pBTM16. To make  $\beta$ -actin and truncated (NT1-4) Gal4-tagged fusion constructs, cDNA was amplified using the clone obtained in a yeast two-hybrid screening as template: NT1-F (5'-GGGAATCCAGAAAATCTGGCACCAC-3'), NT1-R (5'-CCCTCGAGCCTAGAAGCATTGCGG-3'), NT2-F (5'-GGGAATTCCTGTGCTATCCC-3'), NT1-R (5'-CCCTCGAGCCTAGAAGCATTGCGG-3'), NT3-F (5'-GGGAATTCACCGAGCGCGG-3'), NT2-R (5'-CCCTCGAGCCTAGAAGCATTGCGG-3'), NT4-F (5'-GGGAATTCACCATGGCAATG-3'), and NT3-R (5'-CCCTCGAGCCTAGAAGCATTGCGG-3') primers: The products were digested with XhoI and EcoRI and subcloned into pAct2. DNA manipulation and transformation procedures were performed according to Sambrook et al. [12] or according to the protocols recommended by the specific manufacturers.

### Yeast two-hybrid screen (YTHS) and DNA sequencing

The yeast two-hybrid screen [13] of a human fetal brain cDNA library (Clontech Laboratories, Inc., Palo Alto, CA) was performed by using the yeast strain L40 (trp1-901, his3200, leu2-3, ade2 LYS2::(*lexAop*)4-HIS3 URA3::(*lexAop*)8-lac GAL4) and human FBXO25 ( $\Delta$ F) as bait fused to the yeast LexA DNA binding domain in vector pBTM116 (Clontech Laboratories, Inc., Palo Alto, CA). The FBXO25 ( $\Delta$ F) construct does not autoactivate the yeast reporter genes (not shown). The autonomous activation test for HIS3 was performed in minimal medium plates without tryptophan and histidine. Furthermore, the autonomous activation of LacZ was measured by the  $\beta$ -galactosidase filter assay described below. Yeast cells were transformed according to the protocols supplied by Clontech Laboratories, Inc., Palo Alto, CA. The screening was performed in minimal medium plates without tryptophan, leucine, and histidine. The transfected cells were plated in selective medium and the recombinant pACT2 plasmids (Clontech Laboratories, Inc., Palo Alto, CA) of positive clones were isolated and their insert DNAs sequenced with a DNA sequencer (ABI 3100 Perkin-Elmer, Norwalk, CT). Sequence searches in the GenBank database were performed with the BLAST program [14].

### Assay for galactosidase activity in yeast cells

Galactosidase activity in yeast cells was determined by the filter assay method according to Stanley & Fields [13]. Briefly, yeast transformants (Leu+, Trp+, and His+) were transferred onto nitrocellulose membranes, permeabilized in liquid nitrogen, and placed on Whatman 3MM chromatography paper (Whatman LabSales, Hillsboro, OR), previously soaked in Z buffer (60 mM Na<sub>2</sub>HPO<sub>4</sub>, 40 mM NaH<sub>2</sub>PO<sub>4</sub>, 10 mM MgCl<sub>2</sub>, 50 mM 2-mercaptoethanol, pH 7.0) containing 1 mg/ml 5-bromo-4-chloro-3-indolyl- $\beta$ -D-galactoside (X-gal, Invitrogen Life Technologies, Carlsbad, CA). After incubation at 37 °C for 1 h, yeast cells forming dark blue colonies were taken from replica plates for further analysis.

### Cells: Culturing and transient transfection

HEK293T (CRL-11268, American Type Culture Collection, Manassas, VA) cells were grown in Dulbecco Modified Eagle Medium (DEMEM, Sigma-Aldrich, St. Louis, MO)

supplemented with 10% fetal bovine serum (FBS). For transient transfections, expression vectors were introduced into HEK293T (cells at 60–80% confluence) using the calcium phosphate method [15]. After 24 h, the medium was changed to DMEM/FBS containing 10 mM sodium butyrate and the culture maintained for 12 h before lysis. Cultured cells were exposed to 5 µg/ml cytochalasin-D (Sigma-Aldrich) for 24 h and 0.5 µg/ml latrunculin-A (Sigma-Aldrich) for 24 h to inhibit the actin polymerization [16].

### Tandem affinity purification (GF-TAP)

Forty 150 mm plates of HEK293T cells per construct (GST/HA-FBXO25/WT-FLAG, GST/HA-BXO25-ΔF-FLAG and or pcDNA3.1 empty vector) were transfected using the calcium phosphate method [15]. Cells were then washed twice with phosphate-buffered saline (PBS), flash frozen, and lysed in 10 ml of lysis buffer (25 mM Tris, pH 7.4, 225 mM KCl, and 1% Nonidet P-40) supplemented with protease inhibitor mixture SIGMAFAST (Sigma-Aldrich, St. Louis, MO), 2 mM NaF and 1 mM NaVO<sub>4</sub> by vortexing and storing for 2.5 h on ice. The lysates were cleared by centrifugation at 20,000×g for 20 min, at 4°C in an Eppendorf microcentrifuge. Purification of FLAG-tagged proteins and their interacting partners was performed using 150 µl of anti FLAG M2 affinity gel resin (Sigma-Aldrich, St. Louis, MO) for 6 h at 4°C, washing seven times with 500 µl of wash buffer (10 mM Tris, pH = 7.4, 100 mM KCl and 0.5% Nonidet P-40), and eluting with 300 µl of elution buffer I (3XFLAG peptide, Sigma-Aldrich, St. Louis, MO) 0.4 µg/ml, 20 mM Tris, pH = 8.0, 20% glycerol, 100 mM KCl and 1 mM DTT) for 16 h at 4°C with gentle rocking. Supernatants were collected and subjected to pull-down with 40 µl of glutathione Sepharose beads (GE Healthcare, Milwaukee, WI) for 3 h at 4°C with gentle rocking. The beads were then washed seven times with 500 µl of wash buffer and tagged proteins were recovered from the beads using 30 µl of elution buffer II (100 mM glutathione in 100 mM Tris, pH = 7.5).

### Mass Spectrometry

The analysis was performed essentially as described previously [17-20]. The Coomassie blue-stained protein bands were excised from the gel, destained and digested with trypsin (Promega, Madison, WI) in an enzyme-to-substrate ratio of 1:40 (w/w) as described previously [21]. The proteolyzed mixture was analyzed by microcapillary liquid chromatography mass spectrometry (LC-MS/MS) on a hybrid ion trap/FT-ICR mass spectrometer (LTQFT, Thermo, Waltham, MA).

### Immunoblotting

Proteins purified from GF-TAP experiments were transferred to nitrocellulose (GE Healthcare, Milwaukee, WI) and a peroxidase-conjugated secondary antibodies were used to detect the primary antibodies as described elsewhere [10]. Antibodies were visualized by the enhanced chemiluminescence method (Santa Cruz Biotechnology Inc, Santa Cruz, CA).

### Immunofluorescence microscopy

For indirect immunofluorescence, HeLa (CCL-2; American Type Culture Collection, Manassas, VA) and HEK293H (Invitrogen Life Technologies, Carlsbad, CA) cells were grown on glass coverslips in DMEM supplemented with 10% fetal calf serum. The cells were fixed and permeabilized for 10 minutes at room temperature (RT) with PBS containing 2% paraformaldehyde, 0.3% Triton X-100, and 10 µM taxol, then blocked with PBS/2% bovine serum albumin (BSA) containing 5% goat immunoglobulin. Antibody incubations were performed for 1 hour at RT in PBS/2% BSA followed by incubation with Alexa 488- and Alexa 594-coupled secondary antibodies (Invitrogen Life Technologies, Carlsbad, CA). Coverslips were mounted with Prolong gold antifade mounting medium containing DAPI (Invitrogen Life Technologies, Carlsbad, CA). Samples were analyzed with a Leica TCS

SP5 laser scanning confocal microscope (Leica Microsystems, Wetzlar, Germany) as described elsewhere [10]. For quantitative analysis, images were examined by confocal microscopy, and FBXO25 associated nuclear domains (FANDs) and cullin-1 foci were counted; the total number of FANDs, cullin-1 foci, and the number of colocalizing dots were counted in 250 cells from randomly chosen fields in each of four independent microscope slides.

### ***In vitro* transcription assay**

The *in vitro* transcription assay was performed using HeLaScribe<sup>®</sup> nuclear extract *in vitro* transcription system (Promega, Madison, WI) following the manufacturer's protocol using DNA template (AdMLP) described by Hofmann et al [22]. Briefly, HeLaScribe nuclear extract was incubated for 60 min on ice with anti-FBXO25 (0.1 or 0.2  $\mu$ g, [10]) or with  $\beta$ -actin antibodies (2  $\mu$ g, clone C4, Millipore Corp., Billerica, MA). The transcription reaction was then initiated by adding NTPs (400  $\mu$ M UTP, 5  $\mu$ Ci <sup>32</sup>P-CTP, 400  $\mu$ M ATP, and 16  $\mu$ M CTP), DNA template and performed at 30°C for 45 min. The transcription products were purified and separated by 6% acrylamide, 7M urea gel and visualized using FujiFilm FLA3000 phosphorImager (Fuji, Tokyo, Japan).

## **Results**

### **Identification of Proteins that Interact with FBXO25**

In our first attempt to identify FBXO25-interacting proteins we followed the classical tandem affinity purification (TAP) approach [20], whereby the described TAP tag was fused N-terminally to the FBXO25. We observed, however, that this tag construct consisting of two IgG-binding units of protein A from *Staphylococcus aureus*, a cleavage site for the tobacco etch virus (TEV) protease and a calmodulin binding peptide did not efficiently yield the bound FBXO25 upon treatment with TEV protease. These difficulties were circumvented by using an alternative tag originally developed for other purposes during the characterization of the FBXO25 [8]; in this TAP protein construct the FBXO25 was flanked by a glutathione S-transferase and a human influenza hemagglutinin (HA) epitope linked in tandem at the N-terminus, and a FLAG epitope at the C-terminus. Such construct does not interfere with the Ub ligase activity or the nuclear localization of the FBXO25 [8] and performed well in the GF-TAP experiments, allowing the release of the GST/FLAG-TAP (GF-TAP) protein from the anti-FLAG affinity column under mild conditions.

The interaction of FBXO25 with intracellular proteins was assayed in HEK293T cells using the modified GF-TAP protein. These cells are highly transfectable by the calcium phosphate method and express significant amounts of endogenous FBXO25 [8]. HEK293T cells were either transiently transfected with wild-type (WT) FBXO25 or control construct expressing the empty pCDNA3.1 vector alone (mock). The GF-TAP tagged FBXO25 proteins (WT) were purified by two consecutive affinity chromatography rounds under native conditions (Figure 1A). Eluates from the anti-FLAG agarose resin were incubated with glutathione Sepharose beads and proteins bound to the matrix were eluted with glutathione and separated on a 4% - 12% gradient gel by SDS-PAGE (Figure 1B; Supplemental Figure 1).

We purified sufficient amounts of the FBXO25-WT from cell lysates to detect 14 protein bands by Coomassie Blue staining that did not appear in the mock control (Figure 1B). Only a faint IgG light chain band, probably from anti-FLAG gel resin, was observed in the mock control. The protein bands were excised from the gel and subjected to in-gel digestion by trypsin. The resulting peptides were analyzed by microcapillary liquid chromatography - tandem mass spectrometry on a hybrid ion trap/FT-ICR mass spectrometer. One hundred and thirty proteins were identified as FBXO25-WT interacting proteins (A detailed

hyperlinked table with all MS/MS spectra is available in Supplementary Material-Supplemental Table 1). It is noteworthy that, almost all of the major known SCF1-specific subunits were found in this analysis (Table 1).

We further analyzed the FBXO25-interacting proteins using a standard two-hybrid screen (YTHS), a yeast-based genetic assay [13]. Because FBXO25 is present in brain tissue, we screened a human fetal brain cDNA library using an FBXO25- $\Delta$ F mutant as “bait” to minimize the occurrence of interactions with known partner proteins. About a million co-transformed clones were assayed for detection of protein-protein interactions. The transformants were plated without tryptophan, leucine, and histidine (selective minimal medium) and all the grown colonies showing a strong blue color in the subsequent  $\beta$ -galactosidase filter assay were subject to plasmid DNA extraction and sequencing. A total of 65 plasmid DNAs from clones positive for both HIS3 and LacZ reporters were sequenced. As shown in Table 2, only 3 different proteins were identified as FBXO25 interacting proteins and, remarkably, the vast majority (97%) of the transformants were  $\beta$ -actin.

### Validation of Protein Partners

To validate our strategy and confirm the biological significance of the observed FBXO25 interactions, we initially selected for further analysis three known interacting proteins (Table 1) with clear functional implications. We used immunoblotting developed with specific antibodies to detect endogenous Skp1, CUL1, and CAND1 in eluates from the GF-TAP experiments. As shown in Figure 2, GF-TAP tagged FBXO25 protein bound endogenous Skp1. In contrast, these SCF1 components did not copurify with the GF-TAP tagged mutant version of the FBXO25 protein lacking the F-box domain (amino acids 228–266;  $\Delta$ F) which can not interact with Skp1 and thus with other components of the SCF1 complex (Figure 2). It is remarkable that CAND1 also copurified with FBXO25 since CAND1 mediates SCF complex disassembly. Similar results were recently described using a TAP-tagged ANK/F-box protein which purified a SCF complex containing ANK/F-box and CAND1 [23], suggesting the presence of transient forms of SCF1 containing CAND1.

Because FBXO25 is part of a multiprotein complex, and because endogenous Skp1 was reported to be partially found in FANDs [10], we analyzed the CUL1 distribution by immunofluorescence microscopy. Indeed, we found that about 15% of endogenous CUL1, which has never been found in a dot-like nuclear structure, was localized in the FANDs (Figure 3). These results suggest that FANDs contain functional SCF<sup>FBXO25</sup> complex.

In summary, the copurification of endogenous SCF1 components indicates that our modified TAP strategy is a feasible method for identifying of FBXO25 interacting proteins. It remains to be shown whether these newly identified interactions are biologically relevant.

### Nuclear $\beta$ -actin binds FBXO25 and regulates the formation of FBXO25 nuclear bodies

Our observations that  $\beta$ -actin was repeatedly identified by YTHS and that it strongly bound GF-TAP-FBXO25 protein (Figure 1; Table 2), led us to further investigate the FBXO25- $\beta$ -actin interaction. Indeed, the results of the immunoblotting analysis of the material eluted from the affinity resin of a GF-TAP experiment designed to probe the binding of actin to GF-TAP-tagged FBXO25 protein, as shown in Figure 4, corroborates the occurrence of FBXO25- $\beta$ -actin interaction previously observed by other means. To confirm the specificity of this interaction we used anti- $\beta$ -actin antibodies to perform reciprocal immunoprecipitation using nuclear cell preparation and tested for the presence of FBXO25. The results demonstrated that FBXO25 is co-immunoprecipitated with nuclear actin (Supplemental Figure 2).

The YTHS strategy was used to identify the domains involved in the FBXO25- $\beta$ -actin interaction. This study was carried out by retransforming C-terminal deletion constructs of FBXO25 in pBTM16 into the L40 strain containing pACT2 encoding the Gal4- $\beta$ -actin fusion protein. We found that the C-terminus of FBXO25 was necessary to mediate the interaction with  $\beta$ -actin (Figure 5). In addition, prey constructs encoding N-terminally truncated versions of  $\beta$ -actin were also assayed against the recombinant plasmid pBTM116-FBXO25 ( $\Delta$ F). The results revealed that the N-terminus of  $\beta$ -actin was important in mediating the interaction with FBXO25 (Figure 6).

Actin is one of the most abundant cytoplasmic proteins and a basic structural unit of microfilaments (filamentous actin, F-actin), a major component of the cytoskeleton. Actin has also been found in the cell nucleus performing non-structural functions [24,25]. Interestingly, a pool of actin concentrates in immunochemically well-defined nuclear structures, a pattern also observed in FANDs [10]. In keeping with this observation, double-labeling experiments in HeLa cells revealed that FANDs partially colocalized with some of the actin-enriched nuclear structures (Figure 7).

It has been shown that nuclear  $\beta$ -actin regulates the distribution of Cajal bodies in HeLa cells [26] and speckles in HEK293T cells [16]. To further explore the intriguing possibility of actin also being involved in regulating FANDs distribution, we treated HeLa cells with cytochalasin D [27], an inhibitor of actin polymerization and processed them for immunofluorescence confocal microscopy analysis. The proportion of HeLa cells containing FANDs present per nucleus was then estimated (Figure 8). The results showed that cytochalasin D treatment caused a dramatic disruption of FANDs compared with untreated (control) cells. Treatment with latrunculin-A, another actin depolymerizing drug [28], produced very similar results as the cytochalasin-D treatment (Supplemental Figure 3). Importantly, PML bodies were not altered as the result of actin polymerization inhibition, suggesting certain specificity for this phenomenon (Supplemental Figure 4).

As described earlier [22], nuclear  $\beta$ -actin is involved in transcription by RNA polymerase II in mammalian cells. Therefore we analyzed whether FBXO25 is similarly required for transcription using a cell-free system. In this assay, HeLa cell nuclei extracts (HeLaScribe<sup>®</sup>) were incubated with different concentrations of affinity purified rabbit FBXO25 antibodies and transcription was initiated by adding NTPs and DNA template containing the adenovirus major late promoter (AdMLP) fused to a 380-base-pair G-less cassette (Figure 9). The effectiveness of the inhibition was tested in parallel experiments with anti- $\beta$ -actin antibodies [22]. Affinity purified FBXO25 antibodies efficiently inhibited *in vitro* transcription (Figure 9). The effectiveness of the inhibition was tested in parallel experiments with anti-actin antibodies.

As FBPs are essential for the destruction of many regulatory proteins, we hypothesized that FBXO25 may target  $\beta$ -actin for Ub-mediated degradation. To investigate this, we expressed Skp1, CUL1, and Roc1 in HEK293T cells in combination with full-length wild-type (WT) or mutant version of FBXO25 ( $\Delta$ F). FBXO25 protein did not reduce the level of endogenous nuclear  $\beta$ -actin (Supplemental Figure 5).

## Discussion

FBPs are components of E3 Ub ligases responsible for recruitment of an extensive range of substrates of ubiquitination and are, therefore, likely to play important roles in various cellular processes. Indeed, several FBPs, such as FBXL1 and FBXW7, have been shown to be involved in regulating proliferation and differentiation of various cell types [29]. However, the biological functions of the majority of them, including FBXO25, remain

uncharacterized. Thus, elucidating the interactions of FBPs with protein partners of known function is essential in further understanding of their cellular function.

Here we describe a novel TAP tagged protein that is compatible with two-step purification under native conditions. Although two-step TAP strategies have been proven to be successful in avoiding contaminants, it should be cautioned that there is a possibility that some of these proteins bind nonspecifically to FBXO25. We demonstrate the efficiency of the GF-TAP-FBXO25 strategy coupled to mass spectrometry through confirmation of known subunits and regulators of the SCF1 complex. Moreover, this strategy has identified a broad spectrum of potential interacting proteins. Among these,  $\beta$ -actin, which was confirmed genetically by YTHS, is of particular interest for the elucidation of FANDs regulation since  $\beta$ -actin is involved in gene expression [30].

The actin present in the cell nucleus is predominantly in a monomeric globular (G)-actin or short oligomeric form [31,32]. Nuclear actin functions as a key regulatory protein required for RNA transcription, chromatin remodeling, and RNA/protein transport. Importantly, actin is found in the cell nucleus arranged in peculiar foci structures [33]. Some of these actin enriched structures colocalize in part with p80 coilin-positive Cajal bodies [26]. Here, we found a pool of nuclear actin, probably distinct from Cajal bodies [10], which colocalizes and accumulates in FANDs. This argues for multifunctional actin interacting with different components of the cell nucleus.

Cajal bodies are very sensitive to the loss of actin from these structures. Adenovirus infection, which relocates nuclear actin to the periphery of the nucleus, resulted in a disruption of Cajal bodies [26]. Interestingly, actin polymerization is also required for reorganization of the speckles [16]. Our studies showed that FANDs were dispersed and that the FBXO25 redistributed within the nucleoplasm after treatment with drugs that depolymerize actin, suggesting that nuclear actin oligomers and/or polymers play a role in the formation of FANDs and probably in its nuclear function.

In addition, the cell nucleus contains profilin, cofilin, non-muscle myosins, gelsolin, and flightless, proteins known to be modulators of actin dynamics [34-36]. All of them, except profilin, were found in the GF-TAP-FBXO25 eluate (Supplemental Table 1), supporting the idea of a cooperative complex. It remains to be shown whether these interactions regulate FANDs formation.

In summary, the integrated proteomics approach described here to identify protein-protein interactions in FBXO25 represents an applicable strategy for identifying protein complexes from mammalian cells. We provide direct biological, genetic, and biochemical evidence that  $\beta$ -actin physically interacts with FBXO25 and to somehow regulates FANDs formation.

## Supplementary Material

Refer to Web version on PubMed Central for supplementary material.

## Acknowledgments

We specially thank Dr. Wilma A. Hofmann for helpful advice. We also thank Dr. Eduardo B. Oliveira (FMRP-USP, Brazil) and Dr. Emer S. Ferro (ICB-USP, Brazil) for helpful discussion in the preparation of this manuscript. We thank Mrs. Tania Paula Aquino Defina for the sequencing data and Dr. Angela K. Cruz in whose laboratory DNA sequencing was done. Confocal microscopy was performed in the Laboratório de Microscopia Confocal da FMRP-USP. We are also grateful to Mrs. Odete A.B. Cunha and Mrs. Lucia Sakagute for excellent technical support. This study was supported by grant from the FAPESP (2006/58140-9), CNPq (Universal 475393/2009-0 and GENOPROT 42/2009) and FAEPA. Supported in part by a grant from the National Institutes of Health (GM 080587) to PdeL. During these studies, A.O. Manfiolli, A.L.G.C. Maragno and Felipe R. Teixeira were recipients



of FAPESP fellowships; M.M.A Baqui and Sami Yokoo were fellows from the Brazilian agencies CNPq and CAPES, respectively.

## References

1. Frescas D, Pagano M. Deregulated proteolysis by the F-box proteins SKP2 and beta-TrCP: tipping the scales of cancer. *Nat Rev Cancer*. 2008; 8:438–449. [PubMed: 18500245]
2. Hershko A, Ciechanover A. The ubiquitin system. *Annu Rev Biochem*. 1998; 67:425–479. [PubMed: 9759494]
3. Petroski MD, Deshaies RJ. In vitro reconstitution of SCF substrate ubiquitination with purified proteins. *Methods Enzymol*. 2005; 398:143–158. [PubMed: 16275326]
4. Cardozo T, Pagano M. The SCF ubiquitin ligase: insights into a molecular machine. *Nat Rev Mol Cell Biol*. 2004; 5:739–751. [PubMed: 15340381]
5. Duda DM, Borg LA, Scott DC, Hunt HW, et al. Structural insights into NEDD8 activation of cullin-RING ligases: conformational control of conjugation. *Cell*. 2008; 134:995–1006. [PubMed: 18805092]
6. Liu J, Furukawa M, Matsumoto T, Xiong Y. NEDD8 modification of CUL1 dissociates p120(CAND1), an inhibitor of CUL1-SKP1 binding and SCF ligases. *Mol Cell*. 2002; 10:1511–1518. [PubMed: 12504025]
7. Zheng J, Yang X, Harrell JM, Ryzhikov S, et al. CAND1 binds to unneddylated CUL1 and regulates the formation of SCF ubiquitin E3 ligase complex. *Mol Cell*. 2002; 10:1519–1526. [PubMed: 12504026]
8. Maragno AL, Baqui MM, Gomes MD. FBXO25, an F-box protein homologue of atrogin-1, is not induced in atrophying muscle. *Biochim Biophys Acta*. 2006; 1760:966–972. [PubMed: 16714087]
9. Gomes MD, Lecker SH, Jagoe RT, Navon A, Goldberg AL. Atrogin-1, a muscle-specific F-box protein highly expressed during muscle atrophy. *Proc Natl Acad Sci U S A*. 2001; 98:14440–14445. [PubMed: 11717410]
10. Manfiolli AO, Maragno AL, Baqui MM, Yokoo S, et al. FBXO25-associated Nuclear Domains: A Novel Subnuclear Structure. *Mol Biol Cell*. 2008; 19:1848–1861. [PubMed: 18287534]
11. Jin J, Cardozo T, Lovering RC, Elledge SJ, et al. Systematic analysis and nomenclature of mammalian F-box proteins. *Genes Dev*. 2004; 18:2573–2580. [PubMed: 15520277]
12. Sambrook, J.; Fritsch, EF.; Maniatis, T. *Molecular cloning : a laboratory manual*. Cold Spring Harbor Laboratory; Cold Spring Harbor, N.Y.: 1989.
13. Fields S, Song OK. A Novel Genetic System to Detect Protein Protein Interactions. *Nature*. 1989; 340:245–246. [PubMed: 2547163]
14. Altschul SF, Madden TL, Schaffer AA, Zhang JH, et al. Gapped BLAST and PSI-BLAST: a new generation of protein database search programs. *Nucleic Acids Research*. 1997; 25:3389–3402. [PubMed: 9254694]
15. Ausubel, F. M., Brent, R., Kingston, R. E., Moore, D. D., *et al.*, in: *Sons, J. W. (Ed.)*, New York 1997.
16. Wang IF, Chang HY, Shen CK. Actin-based modeling of a transcriptionally competent nuclear substructure induced by transcription inhibition. *Exp Cell Res*. 2006; 312:3796–3807. [PubMed: 17022973]
17. Elias JE, Gygi SP. Target-decoy search strategy for increased confidence in large-scale protein identifications by mass spectrometry. *Nat Methods*. 2007; 4:207–214. [PubMed: 17327847]
18. Eng JK, McCormack AL, Yates JR. An Approach to Correlate Tandem Mass-Spectral Data of Peptides with Amino-Acid-Sequences in a Protein Database. *Journal of the American Society for Mass Spectrometry*. 1994; 5:976–989.
19. Haas W, Faherty BK, Gerber SA, Elias JE, et al. Optimization and use of peptide mass measurement accuracy in shotgun proteomics. *Mol Cell Proteomics*. 2006; 5:1326–1337. [PubMed: 16635985]
20. Shevchenko A, Wilm M, Vorm O, Jensen ON, et al. A strategy for identifying gel-separated proteins in sequence databases by MS alone. *Biochem Soc Trans*. 1996; 24:893–896. [PubMed: 8878870]

21. Shevchenko A, Wilm M, Vorm O, Mann M. Mass spectrometric sequencing of proteins silver-stained polyacrylamide gels. *Anal Chem.* 1996; 68:850–858. [PubMed: 8779443]
22. Hofmann WA, Stojiljkovic L, Fuchsova B, Vargas GM, et al. Actin is part of pre-initiation complexes and is necessary for transcription by RNA polymerase II. *Nat Cell Biol.* 2004; 6:1094–1101. [PubMed: 15502823]
23. Sonnberg S, Seet BT, Pawson T, Fleming SB, Mercer AA. Poxvirus ankyrin repeat proteins are a unique class of F-box proteins that associate with cellular SCF1 ubiquitin ligase complexes. *Proc Natl Acad Sci U S A.* 2008; 105:10955–10960. [PubMed: 18667692]
24. Hofmann WA, de Lanerolle P. Nuclear actin: to polymerize or not to polymerize. *J Cell Biol.* 2006; 172:495–496. [PubMed: 16476772]
25. Louvet E, Percipalle P. Transcriptional control of gene expression by actin and myosin. *Int Rev Cell Mol Biol.* 2009; 272:107–147. [PubMed: 19121817]
26. Gedge LJ, Morrison EE, Blair GE, Walker JH. Nuclear actin is partially associated with Cajal bodies in human cells in culture and relocates to the nuclear periphery after infection of cells by adenovirus 5. *Exp Cell Res.* 2005; 303:229–239. [PubMed: 15652338]
27. Cooper JA. Effects of cytochalasin and phalloidin on actin. *J Cell Biol.* 1987; 105:1473–1478. [PubMed: 3312229]
28. Coue M, Brenner SL, Spector I, Korn ED. Inhibition of actin polymerization by latrunculin A. *FEBS Lett.* 1987; 213:316–318. [PubMed: 3556584]
29. Chen C, Seth AK, Aplin AE. Genetic and expression aberrations of E3 ubiquitin ligases in human breast cancer. *Mol Cancer Res.* 2006; 4:695–707. [PubMed: 17050664]
30. Percipalle P, Visa N. Molecular functions of nuclear actin in transcription. *J Cell Biol.* 2006; 172:967–971. [PubMed: 16549500]
31. Bettinger BT, Gilbert DM, Amberg DC. Actin up in the nucleus. *Nat Rev Mol Cell Biol.* 2004; 5:410–415. [PubMed: 15122354]
32. Pederson T, Aebi U. Nuclear actin extends, with no contraction in sight. *Mol Biol Cell.* 2005; 16:5055–5060. [PubMed: 16148048]
33. Gonsior SM, Platz S, Buchmeier S, Scheer U, et al. Conformational difference between nuclear and cytoplasmic actin as detected by a monoclonal antibody. *J Cell Sci.* 1999; 112(Pt 6):797–809. [PubMed: 10036230]
34. Archer SK, Claudianos C, Campbell HD. Evolution of the gelsolin family of actin-binding proteins as novel transcriptional coactivators. *Bioessays.* 2005; 27:388–396. [PubMed: 15770676]
35. de Lanerolle P, Johnson T, Hofmann WA. Actin and myosin I in the nucleus: what next? *Nat Struct Mol Biol.* 2005; 12:742–746. [PubMed: 16142228]
36. Woolner S, O'Brien LL, Wiese C, Bement WM. Myosin-10 and actin filaments are essential for mitotic spindle function. *Journal of Cell Biology.* 2008; 182:77–88. [PubMed: 18606852]
37. Tipney HJ, Hinsley TA, Brass A, Metcalfe K, et al. Isolation and characterisation of GTF2IRD2, a novel fusion gene and member of the TFII-I family of transcription factors, deleted in Williams-Beuren syndrome. *Eur J Hum Genet.* 2004; 12:551–560. [PubMed: 15100712]
38. Hino S, Kishida S, Michiue T, Fukui A, et al. Inhibition of the Wnt signaling pathway by Idax, a novel Dvl-binding protein. *Mol Cell Biol.* 2001; 21:330–342. [PubMed: 11113207]
39. Assmann EM, Alborghetti MR, Camargo ME, Kobarg J. FEZ1 dimerization and interaction with transcription regulatory proteins involves its coiled-coil region. *J Biol Chem.* 2006; 281:9869–9881. [PubMed: 16484223]

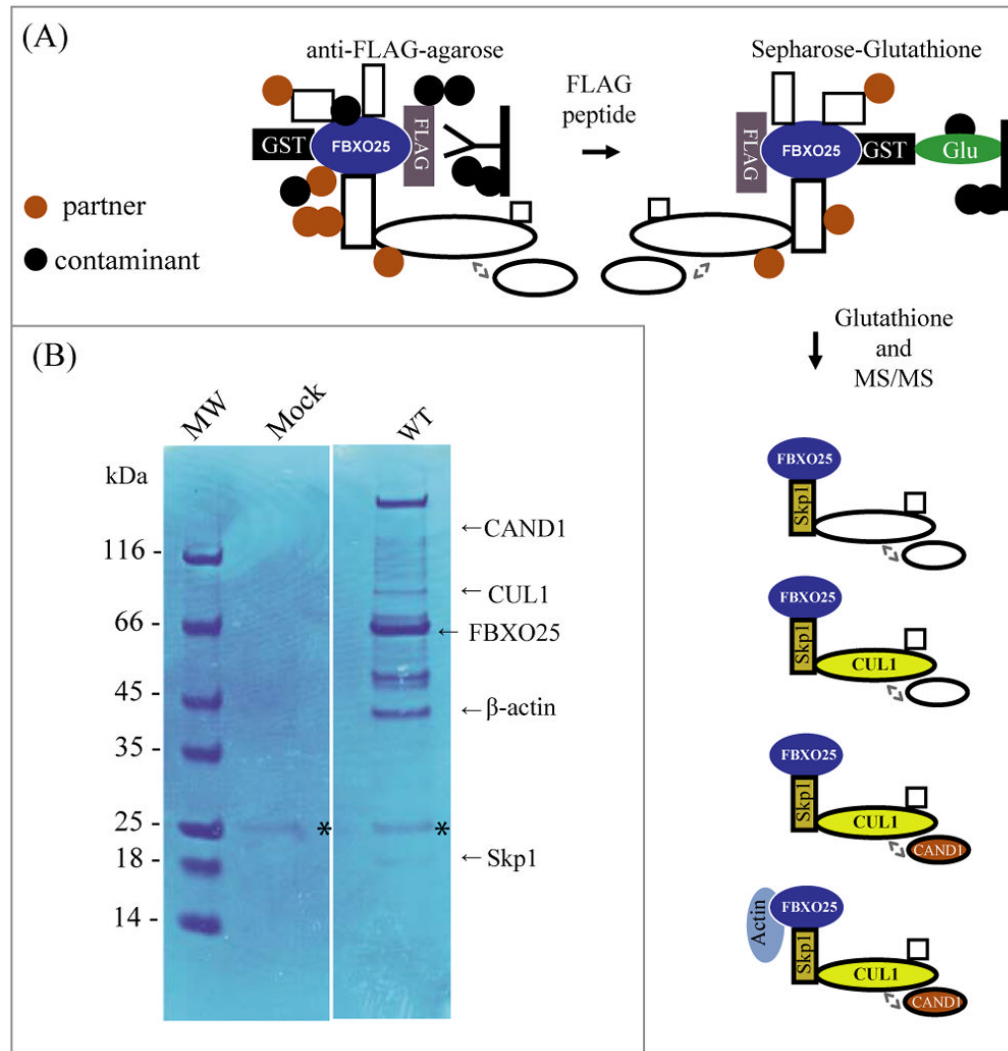


**Figure 1. Tandem affinity purification and its associated proteins from HEK293T cells**  
 (A) Overview of the GF-TAP-FBXO25 protocol. During the first step, GF-TAP-tagged FBXO25 is bound by anti-FLAG M2 agarose beads and released by excess of FLAG peptide. FLAG eluted proteins are then bound to glutathione Sepharose and eluted with 100mM glutathione. In the drawing CAND1 is shown as an associated negative regulator of the SCF complex. (B) Purified proteins were separated using NUPAGE® 4–12% SDS-PAGE and visualized by Coomassie Blue staining. Lane 1, protein marker; lane 2, proteins complexes purified from transfected cells with empty vector (mock); lane 3, protein complexes purified from transfected cells with GST/HA-FBXO25-WT-FLAG. Arrows indicate the positions of FBXO25 (WT) and its interacting proteins as identified by mass spectrometry. Asterisk indicate the IgG light chain. The final data set contains a total of 130 proteins identified (Supplemental Table 1).

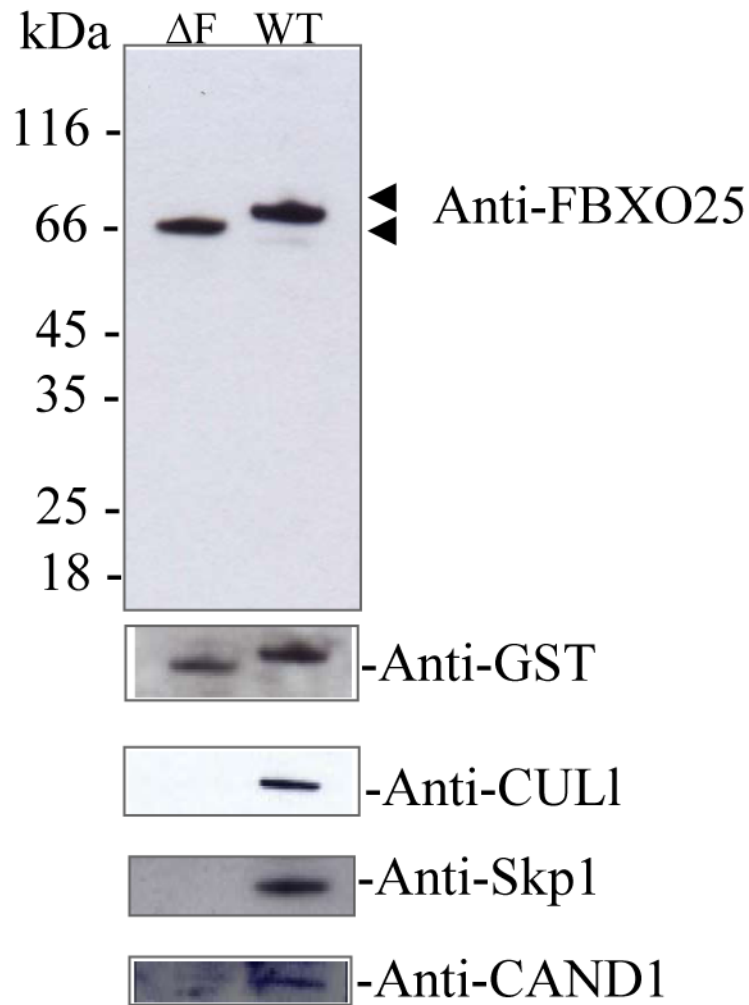


**Figure 2. Validation of the interactions between FBXO25 and proteins from SCF complex identified by the MS**

Approximately 10% of the total eluates from the GF-TAP experiments were subjected to SDS-PAGE (12%), transferred onto nitrocellulose membranes in western blots. FBXO25 mutant lacking the F-box domain ( $\Delta F$ , lane 1) and full-length FBXO25 (WT, lanes 2) complexes were analyzed by the antibodies indicated. Note that Skp1, CUL1, and CAND1 known SCF interacting proteins were not found copurified with FBXO25- $\Delta F$ .

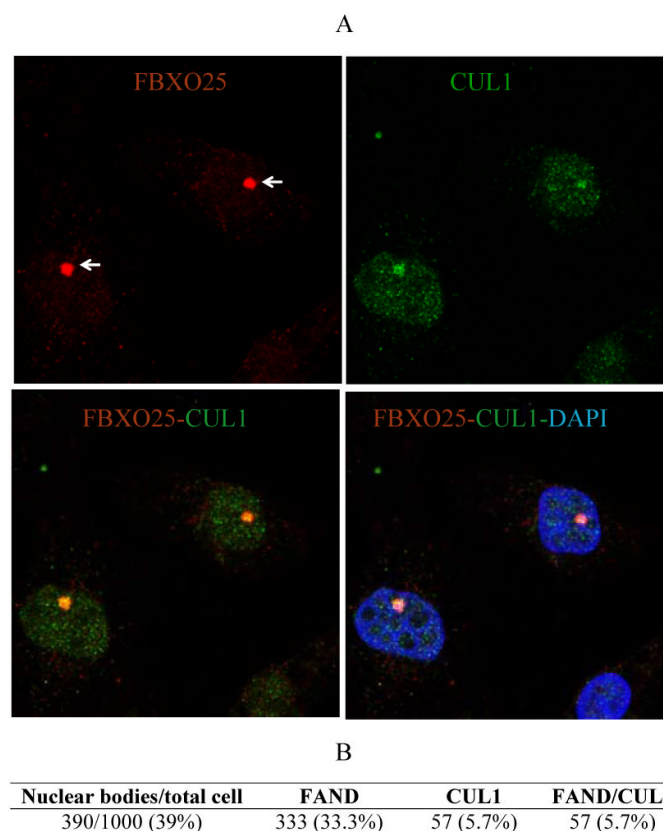


**Figure 3. Colocalization of FBXO25 with CUL1 in nuclei of HeLa cells**

(A) Confocal microscopy of cells double-stained with affinity-purified anti-FBXO25 antibodies and antibodies against CUL1. The proteins labeled in each panel are indicated in the upper left and right of the panel in the relevant color. DAPI was used to stain nuclei. (B) Proportion of cells showing colocalization between FANDs (or FBXO25 bodies, arrows) and CUL1 foci were estimated. Four separate experiments were performed and around 250 cells per slides were analyzed.

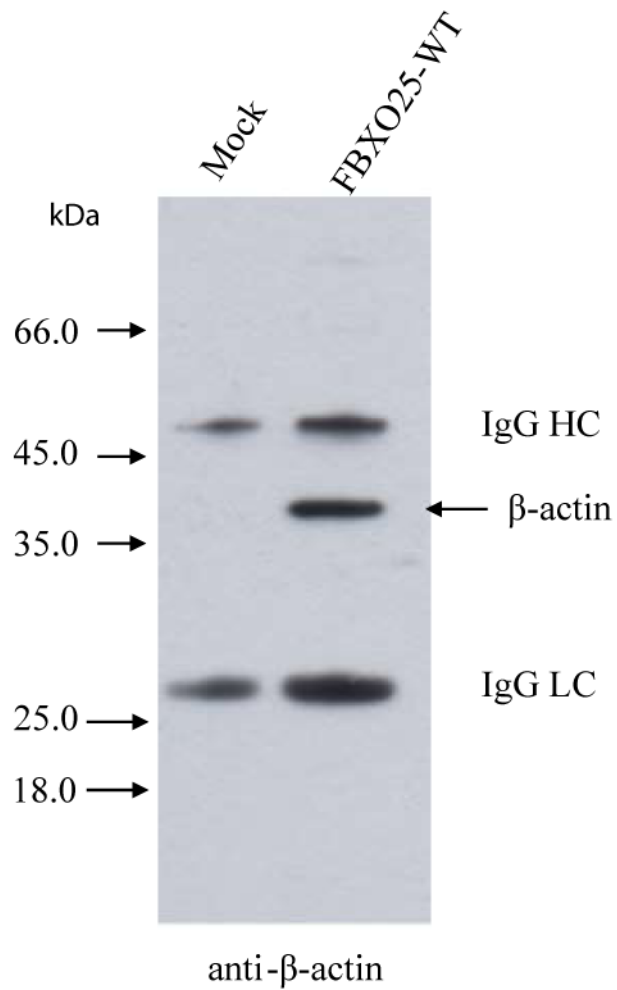


**Figure 4. Validation of interaction between FBXO25 and  $\beta$ -actin identified by the MS**  
Approximately 10% of the total eluates from the GF-TAP experiments were subjected to SDS-PAGE, transferred onto nitrocellulose membranes in western blots. The empty vector (lane 1) and full-length FBXO25 (lane 2) complexes were analyzed by anti- $\beta$ -actin. IgG heavy chain (HC) and light chain (LC) are shown.

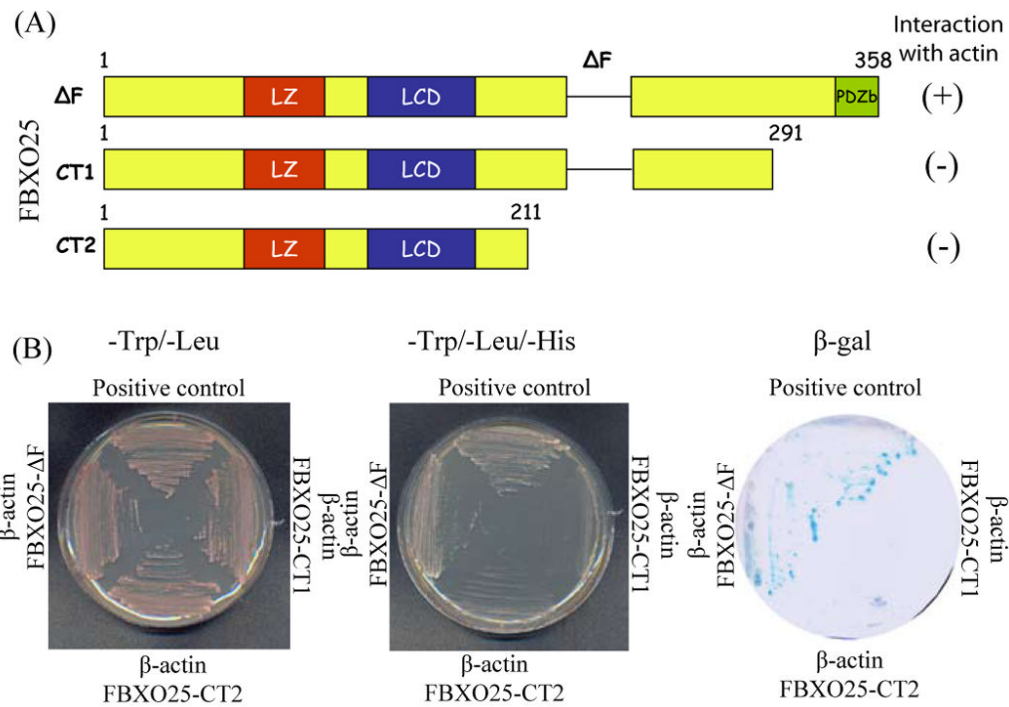


**Figure 5. Mapping of the FBXO25 deletion constructs for activation in the yeast two-hybrid screen**

(A) Schematic drawing of FBXO25 mutant lacking the F-box domain ( $\Delta F$ ) and C-terminally truncated versions of FBXO25 fused to LexA DNA binding domain in plasmid pBTM116. (B) Results of the test for reporters gene activation by different FBXO25 constructs. The L40 yeast strain was cotransfected with the indicated pBTM116-FBXO25 and pACT2- $\beta$ -actin isolate from a human fetal brain cDNA library and plated onto minimal medium without tryptophan and histidine. Activity of reporter genes was determined by growth on selective media (-L/-W/-H) and by galactosidase activity assay. The presence of the plasmid in the L40 cells was verified by growth on plates lacking tryptophan and leucine. pBTM116-FEZ1/pACT2-FEZ2 pair [39] was used as positive interaction control.

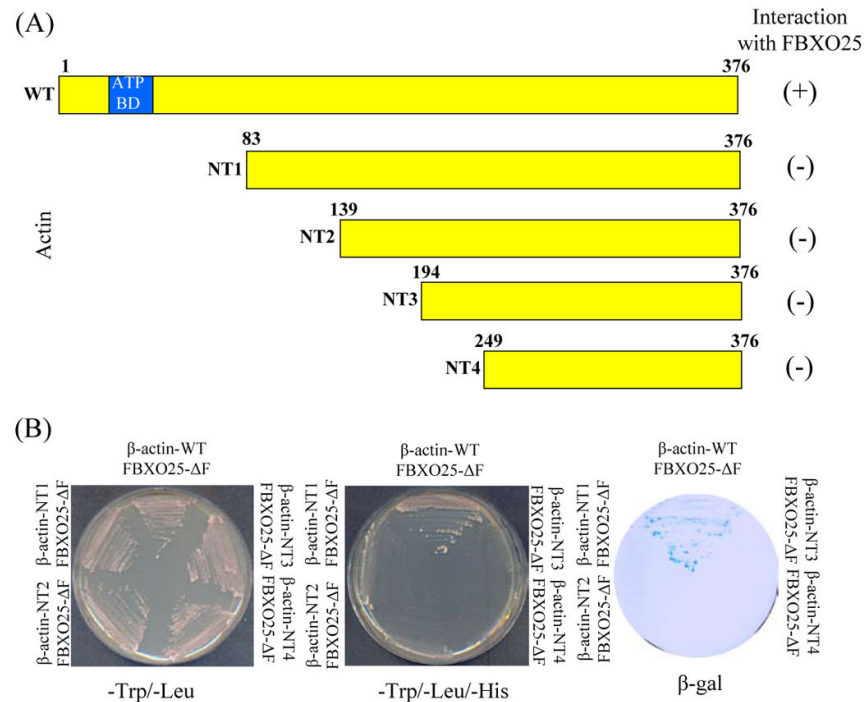


**Figure 6. Mapping of the  $\beta$ -actin deletion constructs for activation in the yeast two-hybrid screen** (A) Schematic drawing of full-length wild-type and N-terminally truncated versions of  $\beta$ -actin fused to Gal4 DNA activation domain in plasmid pACT2. (B) Results of the test for reporter gene activation by different  $\beta$ -actin constructs. The L40 yeast strain was cotransfected with the indicated pACT2- $\beta$ -actin and pBTM116-FBXO25 and plated onto minimal medium without tryptophan and histidine. This test was performed to assay the capacity of these  $\beta$ -actin constructs to activate the reporter genes. The presence of the plasmid in the L40 cells was verified by growth on plates lacking tryptophan and leucine. Actin binding domain (BD) is indicated.



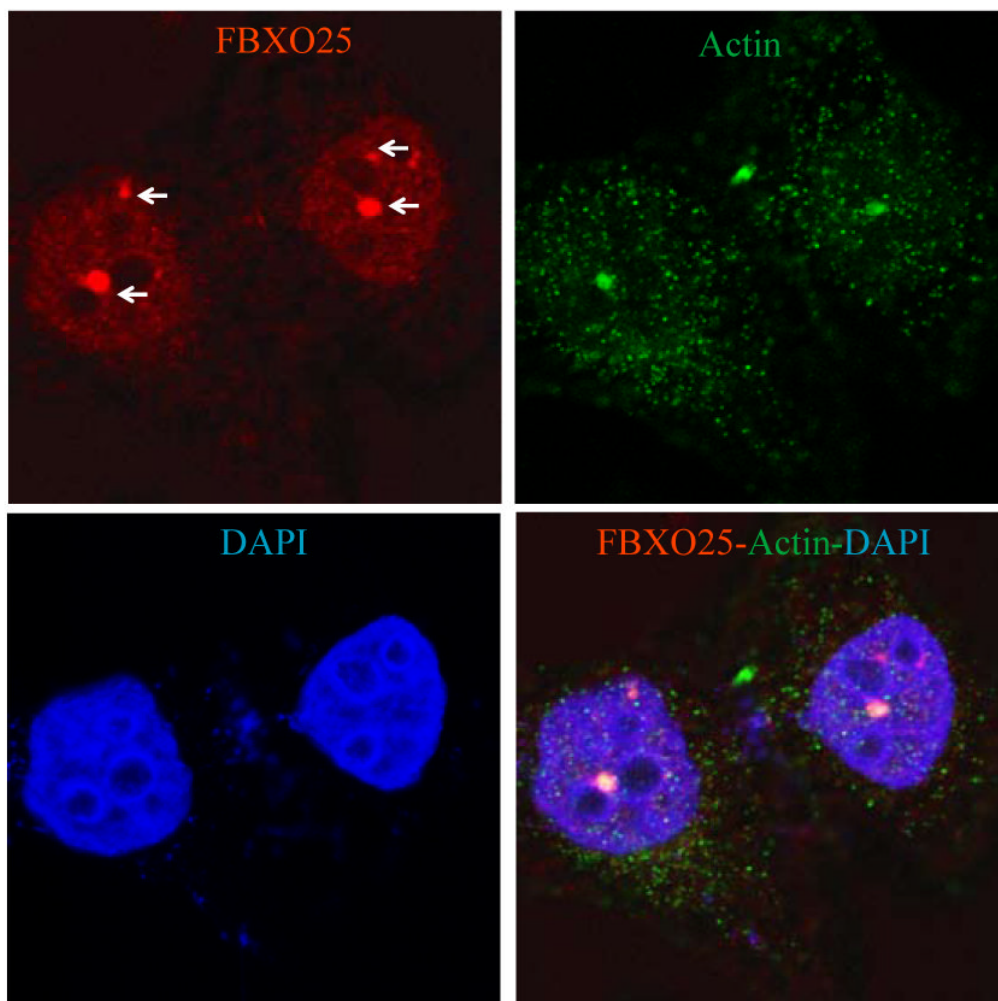


**Figure 7. Partial colocalization of FBXO25 with  $\beta$ -actin in nucleus of HeLa cells**  
Confocal microscopy of cells double-stained with affinity-purified anti-FBXO25 antibodies and antibodies against  $\beta$ -actin. The arrow points to a FAN. The proteins labeled in each panel are indicated in the upper left and right of the panel in the relevant color. DAPI was used to stain nuclei.

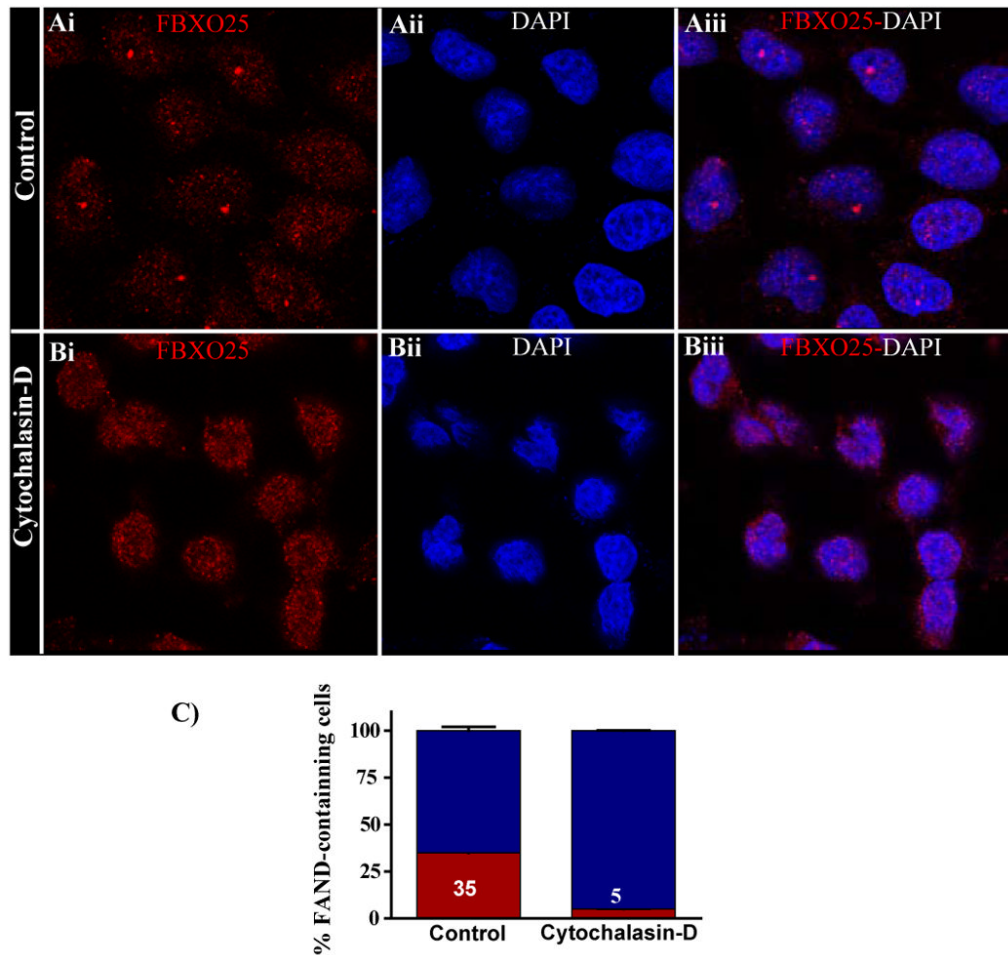


**Figure 8. Inhibition of actin polymerization using cytochalasin-D disrupts FANDs**  
 Confocal microscopy of labeled FBXO25 in untreated and cytochalasin-D-treated (5  $\mu\text{g}/\text{ml}$  for 24 h) HeLa cells are shown. Without cytochalasin-D treatment, FANDs were found in the nucleoplasm (Ai–Aiii). In the presence of cytochalasin-D, the majority of endogenous (Bi–Biii) FANDs disappeared (B). (C) Proportion of cells containing FANDs was estimated. After treatment with cytochalasin-D, the proportion of cells containing FANDs (red) significantly differs from the control population. Four separate experiments were performed, and around 100 cells per slides were analyzed for cytochalasin-D treatment.

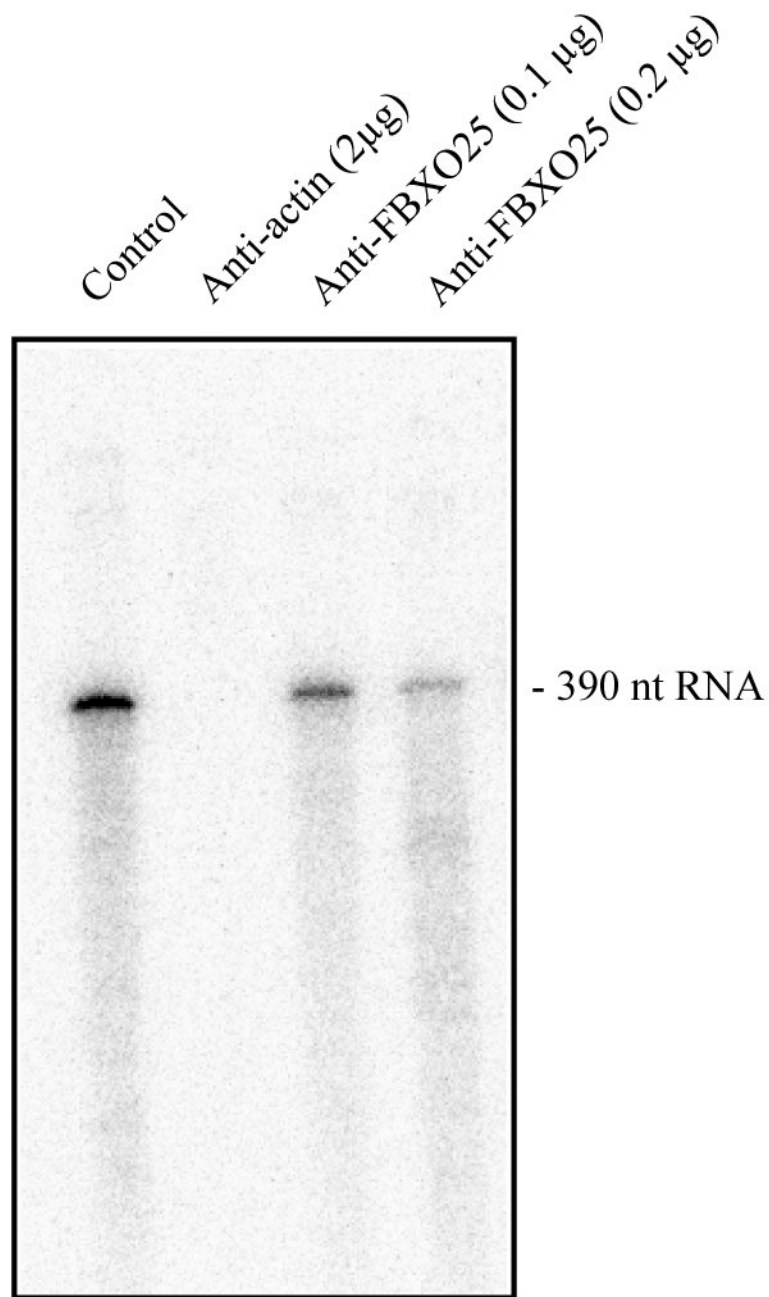


**Figure 9. Antibodies anti-FBXO25 inhibit RNA polymerase II transcription *in vitro***

A HeLaScribe<sup>®</sup> nuclear extract was incubated with anti- $\beta$ -actin or anti-FBXO25 antibodies. The control represents samples that were incubated with antibody diluent only. After incubation for 60 min, transcription was initiated by adding DNA template and rNTPs. The products were subjected to electrophoresis on a 6% denaturing polyacrylamide gel and exposed to a phosphorimaging screen to detect radioactive bands. This experiment was repeated twice.

Table 1

Peptides from FBXO25, Skp1, CUL1, CAND1, and  $\beta$ -actin identified in MS/MS analyses.

CAND1 (EMBL-EBI: IP100100160.3)				
m/z	z	Peptides	Position in Protein	X <sub>corr</sub>
663.78760	2	R.AVAALLTIPEAEK.S	1179 - 1191	2.667
605.76672	2	R.HEM*LPEFYK.T	365 - 373	2.608
772.40698	2	K.ITSEALLVTQQLVK.V	535 - 548	2.568
742.83862	2	K.ISGSILNELJGLV.R.S	730 - 743	2.568
629.24707	2	K.LGTL.SALDILIK.N	668 - 679	2.137
861.86407	2	K.FTISDHPQPIDPLK.N	991 - 1005	2.126
586.67407	2	K.TLEDPLNV.R	1014 - 1023	2.070
743.95496	2	K.EGPAVVGQFIQDVK.N	813 - 826	2.015
CUL1 (EMBL-EBI: IP100014310.3)				
757.79089	2	K.M*DILAQVLQILLK.S	633 - 645	4.911
981.25537	2	R.ESTEFLLQNPVTEYM*K.K	247 - 262	4.159
780.72217	2	K.ESFESQFLADTER.F	230 - 242	3.710
894.97229	2	K.LLETHIHNQGLAAIEK.C	339 - 354	3.673
855.62659	2	K.HQQLLGEVLTQLSSR.F	727 - 741	3.411
1124.73144	2	K.YNALVM*SAFNNDAGFVAALDK.A	377 - 397	3.121
833.33325	2	K.GQTPGGAQFVGLLEYK.R	75 - 90	3.072
1116.46899	2	K.YNALVMSAFNNDAGFVAALDK.A	377 - 397	2.997
521.16315	2	R.M*FQDIGVSK.D	507 - 515	2.948
895.33618	2	R.VQVYLHESTQDELAR.K	275 - 289	2.752
675.36792	2	K.M*YVQTVLVDVHK.K	365 - 375	2.731
737.12897	2	K.QIGLDQIWDLLR.A	14 - 25	2.709
1036.00842	2	K.HLEIFHFQNLDDADK.N	299 - 315	2.634
487.12463	2	R.IQDGLGELK.K	329 - 337	2.616
718.69324	2	K.FYTQQWEDYR.F	118 - 127	2.566
518.64606	2	R.AGIQQVYTR.Q	26 - 34	2.518
667.16626	2	K.MYVQTVLVDVHK.K	365 - 375	2.456

CAND1 (EMBL-EBI: IP100100160.3)				
m/z	z	Peptides	Position in Protein	Xcorr
1111.37231	2	K.NPEEAELEDITLNQVM*VVFK.Y	436 - 454	2.386
980.85632	2	R.ESTEFLLQQNPVTEYM*K.K	247 - 262	2.366
676.50354	2	K.DGEDLMDESVLK.F	106 - 117	2.281
643.25110	2	K.YIEDKDVFK.F	455 - 464	2.247
952.56689	2	R.LVHQNSASDDAEASMISK.L	474 - 491	2.186
897.86658	2	K.KGQTPGGAQFVGLLELYK.R	74 - 90	2.647
576.74609	2	K.LTWLYQLSK.G	579 - 587	2.032
FBXO25 (EMBL-EBI: IP100014310.3)				
633.48407	2	R.LDFSSAIQDIR.R	43 - 53	4.321
1012.09888	3	K.DSGHPCIAADPDSCFTVPSPQHFDL.FK.F	263 - 290	3.774
610.19012	2	K.SQLTSLSGVAQK.N	68 - 79	3.197
609.92322	2	K.SQLTSLSGVAQK.N	68 - 79	3.075
610.32690	2	K.SQLTSLSGVAQK.N	68 - 79	3.020
633.14581	2	R.LDFSSAIQDIR.R	43 - 53	3.011
514.23706	2	K.NYFNILDK.I	80 - 87	2.851
744.60583	2	K.SVLVGNINIWICR.L	123 - 135	2.562
514.23907	2	K.NYFNILDK.I	80 - 87	2.383
633.43774	2	R.LDFSSAIQDIR.R	43 - 53	2.240
633.55469	2	R.LDFSSAIQDIR.R	43 - 53	2.222
514.28241	2	K.NYFNILDK.I	80 - 87	2.070
SKP1 (NCBI- gi 25777711)				
940.41064	2	K.LQSSDGEIFEVDVEIAK.Q	5 - 21	4.412
713.33685	3	K.VDQGTLFELILAANYLDIK.G	94 - 112	3.816
940.95300	2	K.LQSSDGEIFEVDVEIAK.Q	5 - 21	3.371
882.32397	2	K.RTDDIPVWDQEFK.V	80 - 93	3.358
1068.98218	2	K.VDQGTLFELILAANYLDIK.G	94 - 112	3.257
940.32556	2	K.LQSSDGEIFEVDVEIAK.Q	5 - 21	2.869
940.25752	2	K.LQSSDGEIFEVDVEIAK.Q	5 - 21	2.787

CAND1 (EMBL-EBI: IP100100160.3)				
m/z	z	Peptides	Position in Protein	Xcorr
940.34827	2	K.LQSSDGEIFEVDVEIAK.Q	5 - 21	2.212
803.73047	2	R.TDDIPVWDQEFLLK.V	81 - 93	2.034
$\beta$ -actin (EMBL-EBI: IP100021439.1)				
1116.76733	2	K.DLYANTVLSGGTTM*YPGIADR.M	292 - 312	4.019
978.17908	2	R.VAPEEHPVLLTEAPLNPK.A	96 - 113	3.678
1062.34473	3	R.TTGIVMDSGDGVTHIVPIYEGYALPHAILR.L	148 - 177	3.151
759.21936	2	K.QEYDESGPSIVHR.K	360 - 372	2.678
1172.37195	2	R.KDLYANTVLSGGTTMYPGIADR.M	291 - 312	2.558
567.06982	2	R.GYSFTTTAERE	197 - 206	2.499
1116.57044	2	K.DLYANTVLSGGTTM*YPGIADR.M	292 - 312	2.149

**Table 2**

Proteins associated with FBXO25 identified in yeast two-hybrid screen.

Proteins	Number of hits	Function*
$\beta$ -actin	63	[30]
GTF2IRD2	1	[37]
CXXC 4	1	[38]

\* For further details about the interacting protein see the references.